JOURNAL OF SOLID STATE CHEMISTRY 82, 87–94 (1989)

Cation-Deficient Mn, Co Spinel Oxides Obtained by Thermal Decomposition of Carbonate Precursors

J. M. JIMÉNEZ MATEOS, J. MORALES, AND J. L. TIRADO

Departamento de Química Inorgánica e Ingeniería Química, Facultad de Ciencias, Universidad de Córdoba, Córdoba 14004, Spain

Received February 9, 1989; in revised form May 9, 1989

Co, Mn mixed oxides with spinel-related structure are prepared by the thermal decomposition of mixed carbonates under air atmosphere at 400 and 600°C. These oxides are cation-deficient phases with stoichiometries ranging from $MO_{1.333}$ to $MO_{1.6}$ that depend on Mn content and temperature of preparation and show tetragonal to cubic spinel structure as the Co content increases. Additionally, the X-ray diffractograms and electron microscopy data reveal the occurrence of vacancy ordering in a tetragonal superstructure, which is similar to γ-Fe_2O_3 in cubic phases and implies $a' = a$ and $c' = 3c$ for tetragonally distorted spinels.

Introduction

The preparation of mixed oxides with spinel structure by alternative routes to the ceramic method, such as the use of precursor compounds, has been proven to be effective in obtaining ultrafine materials (*1, 2*) that can be converted into cation-deficient phases by thermal treatments. These processes have been extensively studied for the Fe–Mn–O and Fe–Co–O systems by Gillot and co-workers (*3–6*) who used mixed oxalate precursors.

Recently, Rao *et al.* (*7, 8*) proposed the use of carbonate precursors in the preparation of Mn–Co monoxides. The thermal oxidation of these oxides was used to obtain stoichiometric M_3O_4 phases. Due to the multiple oxidation states of Mn and the compositional possibilities of the spinel structure, the carbonate precursor method may be used to prepare cation-deficient spinel-related phases containing Mn in high-oxidation states.

The aim of this work is to study the products of the thermal decomposition of mixed Mn/Co carbonates at low temperatures and nonequilibrium oxidizing conditions. The possible nonstoichiometry and vacancy ordering in these materials are also examined.

Experimental

Mixed carbonates of general formula $Co_{1-x}Mn_xCO_3$ were prepared from the addition of a 1.0 *M* solution of $NaHCO_3$ to a 0.5 *M* solution of Co(II) and Mn(II) in the desired proportions, under a continuous flow of CO_2 (*9*). Mn and Co contents and homogeneity in cation distribution were determined by electron microprobe, X-ray ED analysis. The stoichiometry was confirmed by atomic absorption spectrometry. The average oxidation state of metal ions in the samples was determined by the following procedure. About 50 mg of the samples was dissolved in 5 ml of 0.1 *M* Fe^{2+}, 5 ml of concn H_2SO_4, 5 ml of concn HCl, and 10 ml

0022-4596/89 $3.00

of H_2O, under a continuous flow of Ar, and heated until complete dissolution. After cooling to 20–25°C, 10 ml of H_3PO_4, 25 ml of H_2O, and 1.5 ml of indicator (0.3% diphenilamine in ethanol) were added. The solution was titrated with standard 0.05 *M* K_2CrO_7. Previously, a blank titration was carried out under the same conditions. The difference between both titrations was assigned to the total content in oxidating species (Co(III), Mn(III), and Mn(IV)), and was used to calculated the O/*M* ratios. This procedure cannot be used to determine the content of each oxidating species separately.

X-ray diffraction was carried out with a Siemens D500 diffractometer, using Cu$K\alpha$ radiation monochromated by a graphite crystal. The X-ray line profiles were used in intensity measurements and precision determination of lattice parameters and recorded by step-scan with step sizes of 0.02° 2θ. Si and Co_3O_4 were used as standards in these analyses. Electron micrographs were obtained with a JEOL 200CX apparatus.

DSC and TG curves were obtained with a Mettler TA 3000 apparatus and a Cahn 2000 electrobalance, respectively, under static air atmosphere and heating rates of 8°C/min.

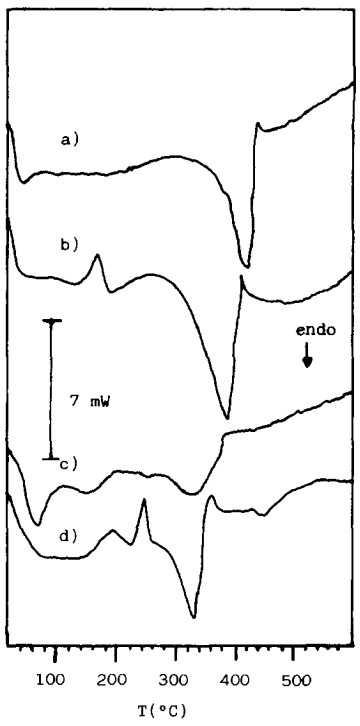

FIG. 1. DSC traces of $Co_{1-x}Mn_xCO_3$ recorded under static air atmosphere: (a) x = 0.677, sample weight (s.w.) = 12.19 mg; (b) x = 0.524, s.w. = 27.47 mg; (c) x = 0.355, s.w. = 12.66; (d) x = 0.000, s.w. = 13.36 mg.

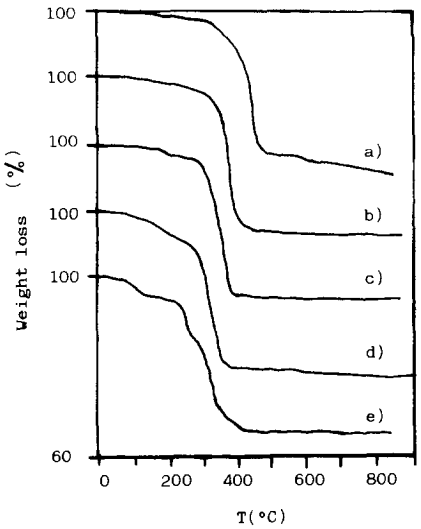

FIG. 2. TG traces of $Co_{1-x}Mn_xCO_3$ recorded under static air atmosphere: (a) x = 1; (b) x = 0.677; (c) x = 0.524; (d) x = 0.355; (e) x = 0.000.

Results and Discussion

The nine samples of Mn, Co mixed carbonates indicated the calcite structure and no other phase was detected by X-ray diffraction. However, the presence of surface hydroxyls and weakly bounded water cannot be discounted, as evidenced by low-temperature endothermal weight loss effects shown by DSC (Fig. 1) and TG data (Fig. 2).

The thermal decomposition of the car-

bonate samples takes place between 300 and 400°C (Figs. 1 and 2), and the decomposition temperature increases with Mn content, in agreement with the literature data (*10*).

The endothermal decomposition effect is the most relevant feature in the DSC traces, recorded under static air atmosphere. The presence of a low-intensity exotherm following this effect can be associated with oxidation reactions, although the possible contribution of recrystallization phenomena to the released heat cannot be discounted. The TG traces (Fig. 2) show a multiple-step continuous weight loss in that temperature interval, thus indicating that the decomposition and oxidation processes occur simultaneously.

The products obtained after 1 hr of thermal treatment above the exothermal effect (400°C) showed the spinel structure by X-ray diffraction (Fig. 3). In these diffractograms some extra lines appear, whose nature will be discussed below. On the other hand, O/*M* ratios determined by chemical analysis (Table I) of the samples prepared at 400°C are higher than 1.5, the expected stoichiometry for τ-sesquioxides, except for $x = 0$ (Co_3O_4 stoichiometry). These values were confirmed from quantitative evaluation of TG data obtained by thermal treatment of the decomposed samples. The TG traces of the products obtained at 400 and 600°C were recorded until a constant weight was reached (ca. 900°C). According to previous research (*13, 14*), the M_3O_4 stoichiometry is reached at this temperature. The complete weight loss was used to calculate the O/*M* ratios in the initial decomposed samples (Table I). It should be noted that Mn(IV) has been found in cation-defective Fe–Mn spinels (*4, 5*) and that Ti, Fe mixed spinels may reach O/*M* ratios higher than 1.5 (*11*). Recently, Feltz and Jäger (*12*) reported an O/*M* = 1.7 in Mn oxides prepared by Mn carbonate decomposition.

Similarly, the samples obtained at 600°C

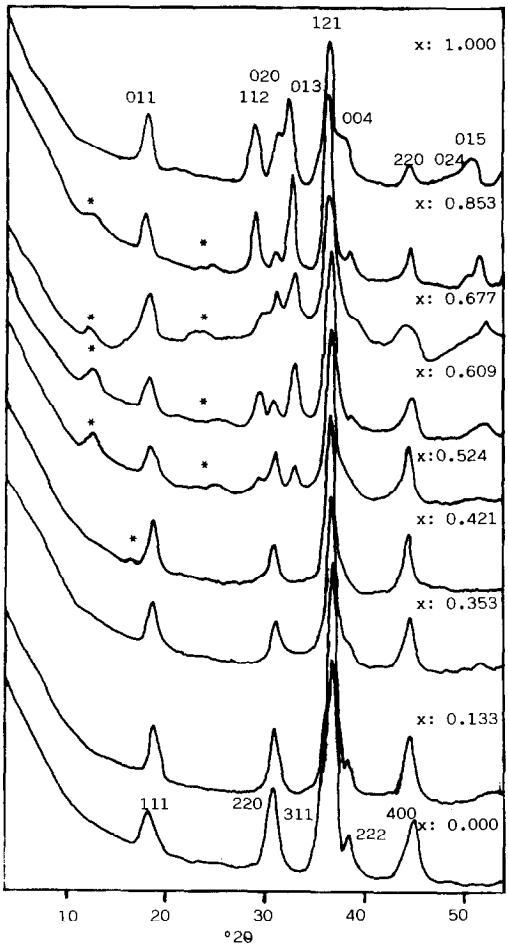

FIG. 3. X-ray diffractograms of the spinel phases obtained by the thermal decomposition of $Co_{1-x}Mn_xCO_3$ at 400°C. Miller indices for $x = 0.000$ and $x = 1.000$ denote cubic and tetragonal spinel reflections, respectively. *, Tetragonal superstructure lines with $a' \approx a$ and $c' \approx 3c$.

also show high O/*M* ratios irrespective of the method of determination (Table I). However, values clearly higher than 1.5 are only obtained for $x > 0.677$. From the X-ray diffraction data (Figs. 3 and 4), the spinels show cubic structure for $x < 0.421$, in agreement with previous research (*13*). For $x > 0.61$ a tetragonal structure was clearly observed which is derived from the Jahn–Teller effect for octahedrally coordi-

TABLE I

CHEMICAL COMPOSITION AND CRYSTALLOGRAPHIC DATA OF Co, Mn MIXED SPINEL OXIDES OBTAINED FROM THE THERMAL DECOMPOSITION OF CARBONATES

T (°C)	x (Mn/M)	O/M chem.	O/M TG	a (Å)	c (Å)	I_{220}/I_{400}	c' [a]	3c
400	1.000	1.598	1.594	5.823	9.554	T[b]	—	—
	0.853	1.586		5.855	9.436	T	27.42	28.31
	0.677	1.599	1.592	5.854	9.430	T	27.86	28.29
	0.609	1.593		5.851	9.426	T	27.64	28.28
	0.524	1.550	1.552	8.183		0.682	24.76	24.55
	0.421	1.558		8.168		0.761		24.50
	0.353	1.529	1.535	8.151		0.627		24.45
	0.133	1.516		8.153		0.666		24.48
	0.000	1.333	1.333	8.087		1.290	—	—
600	1.000	1.583	1.583	5.78	9.33[c]	T	—	—
	0.853	1.570		5.708	9.308	T	27.42	27.93
	0.677	1.505	1.503	5.786	9.302	T	27.64	27.91
	0.609	1.499		5.798	9.025	T	27.26	27.07
	0.524	1.500	1.470	8.355		1.707	27.84	25.06
	0.421	1.435		8.300		1.312	25.03	24.90
	0.353	1.362	1.374	8.300		1.188	24.92	24.90
	0.133	1.342		8.151		1.296	24.23	24.45
	0.000	1.333	1.333	8.085		1.310	—	—

[a] Superstructure c' parameter computed from 004 and 114 superstructure lines for tetragonal spinels and 110 superstructure lines for cubic spinels.

[b] T, tetragonal phases.

[c] From Ref. (*22*).

nated Mn(III). Previous research (*13, 14*) showed that the critical content of Mn(III) ions in the octahedral sites was about 60% to reach a significant tetragonal distortion of the oxides containing this d^4 ion. The results in Table I are in agreement with these conclusions. For $0.421 \leq x \leq 0.610$, according to previously proposed phase diagrams (*14*), the tetragonal structure should be expected although with a small distortion ($c/a \approx 1$; pseudocubic T_1 spinels). The remaining tetragonal spinels could be considered T_2-type according to (*14*).

If the unit cell parameters a of the cubic spinels (Table I) are compared for samples obtained at 400 and 600°C, larger values are observed at 600°C, probably due to the lower vacancy content at this temperature. However, for both sets of samples, the a parameters increase with Mn content, simultaneously with the increase in O/M ratio. This implies that the cation radius has a stronger effect on the unit cell parameter than vacancy content, although both effects are present, especially at 600°C.

The extra lines observed in the X-ray diffraction patterns (Figs. 3 and 4), that could not be ascribed to an M_3O_4 tetragonal or cubic spinel phase, are not indexable for any other phase in the Mn–O, Co–O, or Mn–Co–O system. Additionally, these lines become more intense as the preparation temperature of the oxide increases. Thus, at 600°C, crystallinity is higher and O/M ratios are closer to 1.5. This may indicate the presence of a superstructure originated by vacancy ordering in a similar way as γ-Fe_2O_3 (*15–17*). In this respect, it

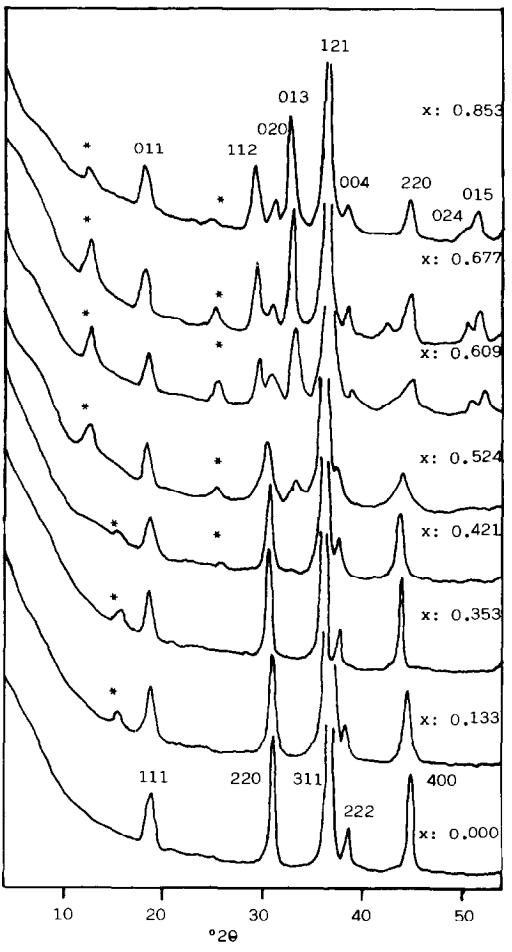

FIG. 4. X-ray diffractograms of the spinel phases obtained by the thermal decomposition of $Co_{1-x}Mn_x$ CO_3 at 600°C. Miller indices and * have the same meaning as in Fig. 3.

should be noted that vacancy ordering has been detected by IR data in mixed oxides Fe–Mn–O (*6*). However, superstructure in γ-Mn_2O_3 (*18, 19*) has not been observed, and the oxidized Mn_3O_4 sample prepared in the present work did not show any extra lines. This fact implies that the presence of cobalt in the oxide is a prerequisite for the occurrence of vacancy ordering phenomena.

A careful examination of the I_{220}/I_{400} intensity ratio in the cubic spinels obtained from mixed carbonates gives additional information. This ratio is dependent on the degree of tetrahedral to octahedral cation occupation (*20, 21*) in spinel-related structures. From the results in Table I, it is evident that the I_{220}/I_{400} ratio is smaller at 400°C and increases markedly at 600°C, where stoichiometry is between M_3O_4 and M_2O_3. This implies that the vacancies tend to occupy tetrahedral sites at 400°C. As Co content and the oxidation state are high, only Co(III), Mn(III), and probably Mn(IV) should be found. Both trivalent ions have a high tendency to occupy octahedral sites due to their high CFSE in this crystal field, thus displacing the vacancies to tetrahedral sites. An additional consequence of this behavior is that the vacancies cannot be ordered with a superstructure similar to that found in γ-Fe_2O_3 (*16*).

On the other hand, at 600°C the lower metal oxidation state may involve Co(II) ions and reduction of a few Mn(IV). These ions are less favorably placed in octahedral sites than Co(III). The high I_{220}/I_{400} ratios are in agreement with this assumption. If a vacancy ordering in octahedral position, similar to γ-Fe_2O_3, is assumed, the resulting Miller indices of the extra reflections in Fig. 4 can be generated, being 110 and occasionally the less intense 210 and 213; these agree well with a tetragonal superstructure with $c' \approx 3a$ (the experimental c' values obtained from superstructure lines are compared with $3c$ in Table I). The electron micrographs of the spinels obtained by thermal decomposition of carbonates are shown in Fig. 5. For cubic spinels at 400°C (Fig. 5a), the micrographs show small particles of nonuniform size (ca. 100 Å) with lattice fringes that can be assigned to (111) and (220) planes. In contrast, at 600°C (Figs. 5b and 5c), the particles increase their size (ca. 600 Å) considerably and show additional contrast effects evidenced by the 6.23 Å fringes that can be indexed in

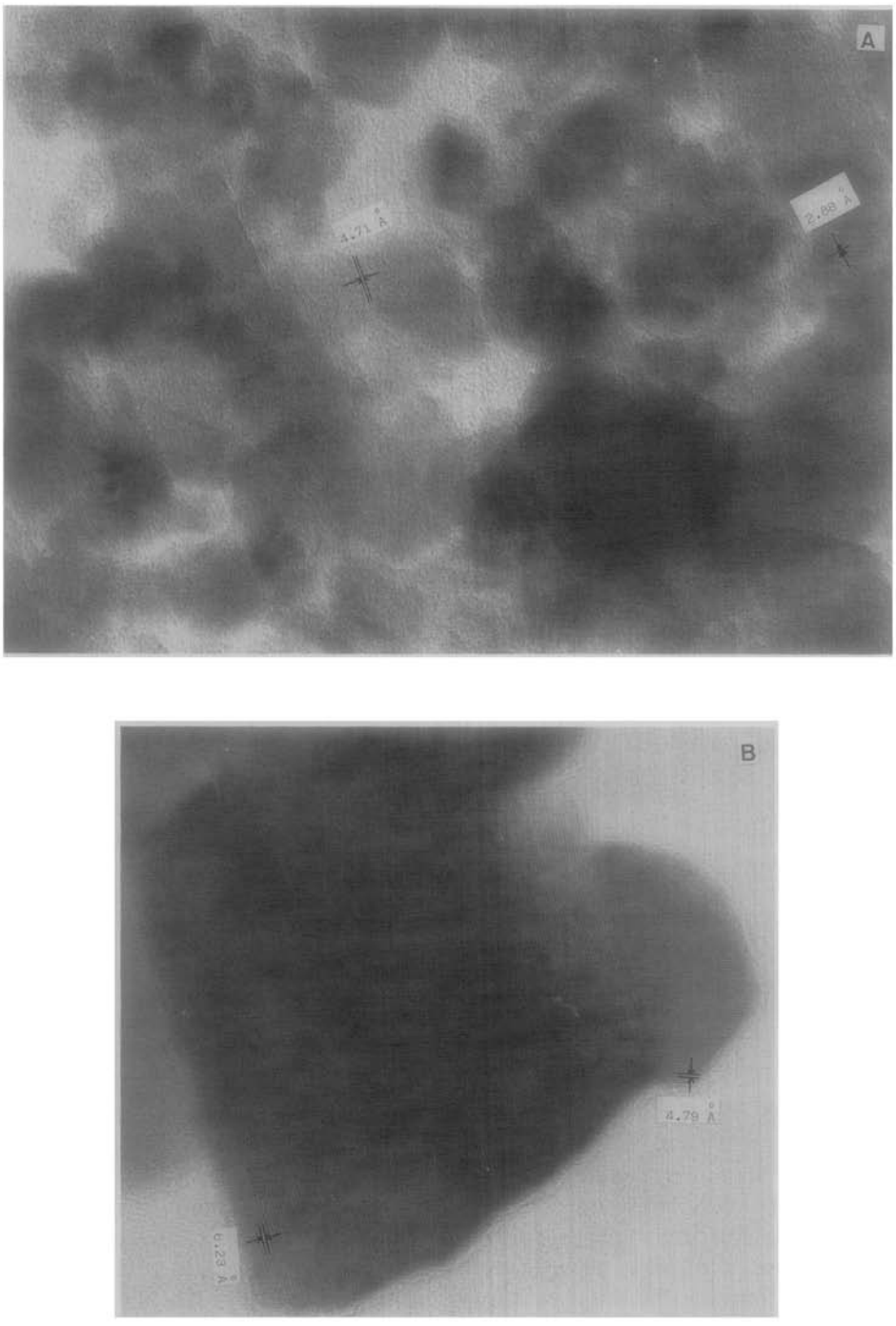

FIG. 5. Electron micrographs of the sample with $x = 0.353$ decomposed at 400°C (a) and 600°C (b and c).

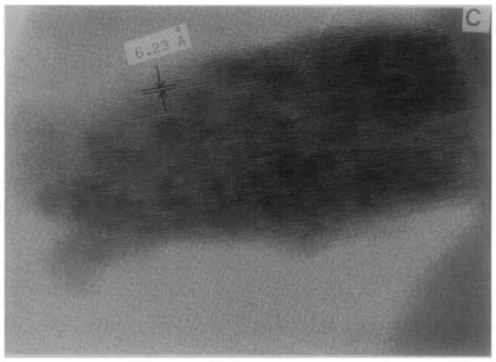

FIG. 5—*Continued*

the tetragonal superstructure as (110) lattice planes. These fringes show a high level of distortion including dislocations and coherent twin boundaries probably reflecting the difficulty in vacancy ordering in extended domains. The powder electron diffraction patterns of these samples showed the same effects as the X-ray diffraction data, including the superstructure effects. Single-crystal electron diffraction studies could not be carried out due to the small size of the particles and the difficulty in the dispersion of the samples.

On the other hand, the X-ray diffraction extra lines for tetragonal spinels (Figs. 3 and 4) can be assigned to the presence of a vacancy ordering superstructure as in the cubic spinel case. In these spinels, the vacancy ordering is also along the *c*-axis, with new unit cell parameters $a' \approx a$ and $c' \approx 3c$ (see Table I), where a and c are the tetragonal unit cell parameters of the $I4_1/amd$ spinel structure (Mn_3O_4 structure (*22*)). The Miller indices for the extra diffraction lines would be 004 and 114. A superstructure of this type has not been found for γ-Mn_2O_3 (*19*) or for the Mn–Co–O system (*23*). From the above results, it can be concluded that the presence of cobalt is necessary for ordering of vacancies in both tetragonal or cubic spinel Co, Mn oxides.

Although the powder X-ray diffraction data do not allow a detailed examination of such a superstructure, it should be noted that the similarity between X-ray diffraction patterns of γ-Fe_2O_3 and $LiFe_5O_8$ patterns (*24*) suggested that cation vacancies were ordered in the octahedral 16d sites of the $Fd3m$ spinel structure. For a tetragonally distorted spinel, the unit cell is now body centered (I), and the cations in distorted octahedral sites occupy 8d equivalent positions of the $I4_1/amd$ group. No other mixed Mn oxide equivalent to Li Fe_5O_8 with a tetragonal structure has been described; thus the manner in which the vacancies are distributed is less clear. However, γ-Fe_2O_3 belongs to the $P4_32_12$ space group, where only one set of 4a equivalent positions are partially occupied by Fe(III) (*16*). The complete occupancy is reached every third 4a site along [001]. For the tetragonal spinels, the ordering of vacancies in a superstructure with a $c' \approx 3c$ may indicate that the 8d equivalent positions in the $I4_1/amd$ space group may split into two groups of multiplicity 4, thus leading to a similar ordering. The final space group cannot be easily determined, but it is probable that the symmetry will be lowered by vacancy assimilation in the observed superstructure.

Acknowledgments

The authors acknowledge CICYT and PFPI for financial support.

References

1. A. ROUSSET, F. CHASSAGNEUX, AND J. PARIS, *J. Mater. Sci.* **21,** 3111 (1986).
2. L. R. CLAVENNA, J. M. LONGO, AND H. S. HOROWITZ, U.S. Patent 4060500 (1977).
3. B. GILLOT, F. JEMMALI, AND A. ROUSSET, *J. Solid State Chem.* **50,** 138 (1983).
4. B. GILLOT, M. EL GUENDOUZI, P. TAILHADES, AND A. ROUSSET, *React. Solids* **1,** 139 (1986).
5. B. GILLOT, M. EL GUENDOUZI, AND A. ROUSSET, *J. Solid State Chem.* **68,** 285 (1987).

6. B. GILLOT, M. EL GUENDOUZI, M. LAARJ, P. TAILHADES, AND A. ROUSSET, *J. Mater. Sci.* **23,** 3342 (1988).
7. C. N. R. RAO AND J. GOPALAKRISHNAN, *Acc. Chem. Res.* **20,** 228 (1987).
8. C. N. R. RAO, J. GOPALAKRISHNAN, K. VIDYASAGAR, A. K. GANGULI, A. RAMANAN, AND L. GANAPATHI, *J. Mater. Res.* **1,** 280 (1986).
9. K. VIDYASAGAR, J. GOPALAKRISHNAN, AND C. N. R. RAO, *Inorg. Chem.* **23,** 1206 (1984).
10. R. C. MACKENZIE, "Differential Thermal Analysis," Academic Press, London (1982).
11. B. GILLOT AND F. JEMMALI, *Mater. Chem. Phys.* **15,** 557 (1986).
12. A. FELTZ AND M. JÄGER, *React. Solids* **6,** 119 (1988).
13. S. NAKA, M. INAGAKI, AND T. TANAKA, *J. Mater. Sci.* **7,** 441 (1972).
14. YU. V. GOLIKOV, S. YA. TUBIN, V. P. BARKHATOV, AND V. F. BALAKIREV, *J. Phys. Chem. Solids* **46,** 539 (1985).
15. K. HANEDA AND A. H. MORRISH, *Solid State Commun.* **22,** 779 (1977).
16. C. GREAVES, *J. Solid State Chem.* **49,** 325 (1983).
17. M. BOUDEULLE, H. BATIS-LANDOULSI, CH. LECLERCQ, AND P. VERGNON, *J. Solid State Chem.* **48,** 21 (1983).
18. JCPDS, Powder Diffraction File 6-540 (1950).
19. JCPDS, Powder Diffraction File 18-803 (1965).
20. B. BERTAUT, *C. R. Acad. Sci. Paris* **230,** 215 (1950).
21. G. D. RIECK AND F. C. M. DRIESSENS, *Acta Crystallogr.* **20,** 521 (1966).
22. JCPDS, Powder Diffraction File 24-734 (1972).
23. JCPDS, Powder Diffraction Files 18-408, 18-409, and 18-410 (1965).
24. P. B. BRAUN, *Nature (London)* **27,** 1123 (1952).